Development of balloon-borne hard x-ray telescope using Pt/C mutilayer supermirror

Y. Ogasaka, K. Tamura, K. Haga, T. Okajima, S. Ichimaru, S. Takahashi,
A. Gotou, H. Kitou, S. Fukuda, H. Kunieda[a], Y. Tawara, K. Yamashita, Y. Tsusaka[b],
P. J. Serlemitsos[c], Y. Soong[c], K.-W. Chan[c], S. Owens[c], F. Berendse[c], and J. Tueller[c]

Dept. of Physics, Nagoya University, Nagoya, Japan
[a]The Institute of Space and Astronautical Science, Sagamihara, Japan
[b]Himeji Institute of Technology, Hyogo, Japan
[c]NASA Goddard Space Flight Center, Greenbelt, MD, USA

ABSTRACT

High sensitivity hard X-ray data by means of focusing optics is crucially important to investigate active galaxies and cluster of galaxies. We have developed focusing telescopes with platinum-carbon multilayer coatings. The energy band is broadened by multilayers with graded periodic length, so called *'Supermirrors'*. We were successful to obtain hard X-ray images in the energy band from 25 to 40 keV with a demonstration model of telescope with 20 mirror shells of supermirrors. The flight model of supermirror telescope is now in production for balloon flight in the summer of 2000. The current status of the balloon mission and future application of supermirror technology is discussed.

Keywords: x-ray telescope, multilayer, hard x-ray optics

1. INTRODUCTION

1.1. Telescope observations in hard X-ray region

In the hard X-ray region, there has been no telescope imaging observation achieved so far. In X-ray astronomy, hard X-ray observations above 10 keV are important to find out many X-ray emitting objects obscured by thick absorption material, sometimes thicker than 10^{24} H atoms cm^{-2} in terms of column density. They have crucial importance in the investigation of star forming regions, active galaxies, and the Cosmic X-ray Background. Mapping observations in such energy range also make clear the distribution of non-thermal components of extended objects, such as super nova remnants and clusters of galaxies. It is because non-thermal emission becomes dominant over the thermal component in higher energies.

The high-throughput X-ray telescopes on board the *ASCA* satellite (Serlemitsos *et al.* 1995) expanded the high energy limit of X-ray imaging up to 10 keV, employing tightly nested thin-foil mirrors. This type of optics has advantages in hard X-ray applications because photon statistics becomes severer so large throughput is eagerly desired. However, reflection of hard X-rays require much shallower incidence angles as long as ordinary mono-layer reflecting surface is employed. This is not adequate since aperture efficiency, thus throughput, is greatly reduced.

1.2. Supermirror technology and hard X-ray focusing optics

The principle of X-ray reflection by mono-layer mirror is a total external reflection. The typical high energy limit is around 10 keV with incidence angles around 0.5 deg in the case of *ASCA* XRT for example. Above the critical energy, X-rays start to penetrate into the material and can be reflected by the interference of periodic structures like crystal lattice or multilayers. Multilayer reflecting surface has the advantage to enhance reflectivity beyond the critical energy, although its energy bandwidth is usually narrow under the constraint of the Bragg condition.

To broaden the sensitive energy band, multilayer with graded periodic length, so called *supermirror*, is suitable. The energy bandwidth of supermirror is a superposition of narrow energy response by each layer pairs under their own Bragg conditions. After intensive studies, we have chosen a design method called "block method", where the gradient of periodic length is not continuous but is expressed as a several blocks of constant-period multilayers. The block method has a great advantage of less number of layers than continuously graded periods to get high reflectivity and flat-top energy response in wide energy range. Detailed discussion is described by Yamashita *et al.* (1998a) and the references therein.

Yasushi Ogasaka: E-mail: ogasaka@u.phys.nagoya-u.ac.jp

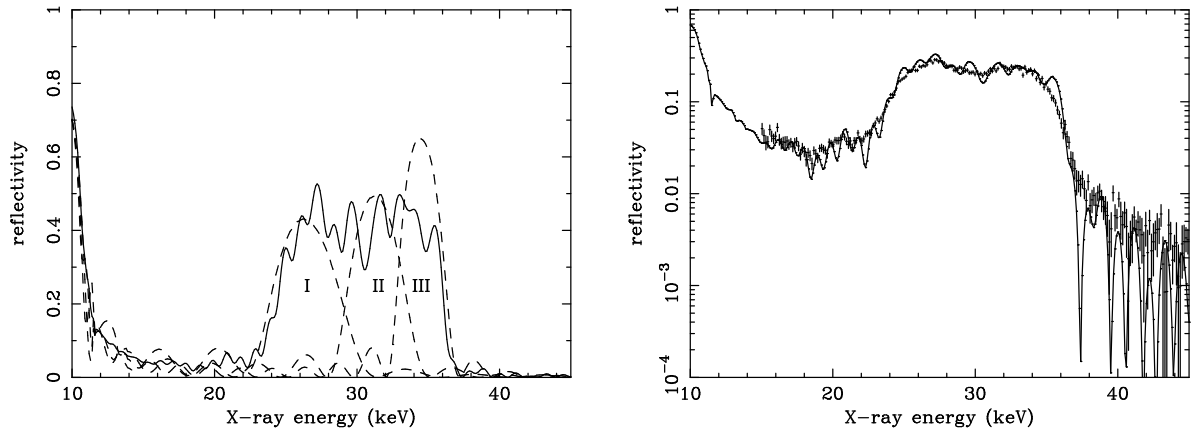

Figure 1. Model reflectivity of Pt/C 3 block supermirror (left) as described in the text for the incidence angle of 0.3 deg. The dashed curves with numbers are the reflectivities of each block. As a consequence of interference and photoelectric absorption, stacked supermirror shows the reflectivity shown with the solid curve. The right panel is a measured reflectivity (dots with error bars) of the supermirror, overlaid with model calculation (solid line). Note that the assumed interfacial roughness is 0 nm for the left panel, while 0.5 nm is used for the right panel to fit the data.

2. DESIGN AND FABRICATION OF SUPERMIRROR

2.1. Supermirror design

The supermirror is a stack of multilayers with different sets (blocks) of periodic length (d) and number of layer pairs (N). The peak reflectivity (R), peak energy (E) and the energy bandwidth(δE) of the Bragg peak of each block are functions of d, N, and the angle of incidence (θ). Here, N is optimized so that the integrated reflectivity $R \times \delta E$ is maximized with possible smallest number. For given energy range of interest, d and N for each block are then determined so that reflectivities from each block fill the energy band without gaps or unnecessary overlaps. Another key parameter is a ratio(Γ) of thickness of heavy element (d_H) to d. It does not have much influence on first order Bragg peak, but higher order peaks are largely affected. Our current design adopts the value of $\Gamma = 0.4$ to enhance first and second order Bragg peaks. The detail of the model calculation and the optimization of supermirror design are described by Yamashita *et al.* (1998b).

The left panel of figure 1 shows an example of model reflectivity of a supermirror consisting of three multilayer blocks. The structures of the blocks are d = 5.0–4.6, 4.0 and 3.6 nm and N = 5, 8 and 13, from the first (vacuum side) block to the bottom (substrate side). Note that the periods of the first block are not constant but graded to obtain smooth reflectivity curve as a result of superposition. Platinum-carbon combination is chosen to obtain the highest peak reflectivity with least number of layer pairs. Long term chemical stability and easiness of thin film deposition are also preferable characteristics of platinum.

2.2. Hard X-ray characteristics of demonstration model

In order to justify the validity of supermirror application to hard X-ray telescope, we had carried out a demonstrational experiment. The three block supermirror described above was deposited on epoxy-replicated conical foil mirror produced for *ASTRO-E* X-Ray Telescope (XRT). The deposition of Pt/C supermirror was done with the magnetron DC sputtering system at Nagoya University. The system is specially designed to fabricate multilayers on the inner surfaces of cylindrical mirror shells of radii from 100 through 250 mm. The detail of the system is described by Tawara *et al.* (1997) and the references therein. Hard X-ray reflectivity of the supermirror was measured with pencil beam reflectometer for 10–45 keV continuum X-rays, as shown in the right panel of figure 1. As can be seen from the figure, a flat-top reflectivity of about 30% in 25–35 keV band was obtained. Overlaid model calculation assumes interfacial roughness (Debye-Waller factor) of 0.5 nm which is consistent with the value intrinsic to the substrate foil mirror.

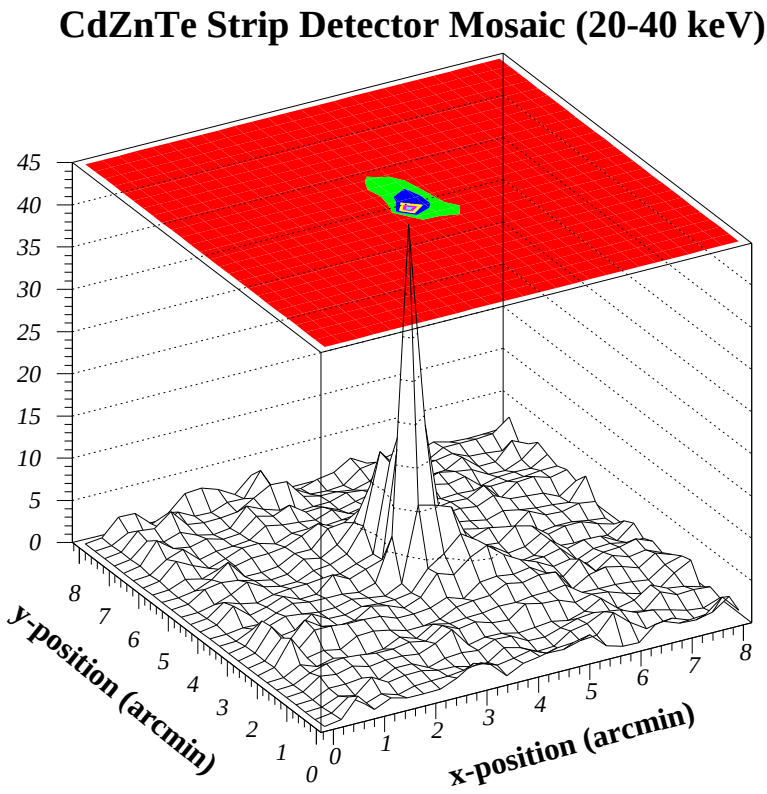

Figure 2. Focused point-source image for 25–40 keV X-rays taken with CdZnTe strip detector of 0.5mm (0.36 arcmin) position resolution.

Ten pairs of *ASTRO-E* foil mirrors were coated with such supermirrors, and were installed into *ASTRO-E* XRT flight housing to test their imaging characteristics. The radii of the foil mirrors are around 100 mm and the focal length is 4.75 m, thus the angles of incidence are around 0.3 deg. The telescope was illuminated by continuum X-rays up to 40 keV. Figure 2 shows the focused image taken with CdZnTe two-dimensional strip detector in 20–40 keV band. Low energy image was also measured with X-ray CCD camera for monochromatic 4.51 keV (Ti-Kα) X-rays. The half-power diameter (HPD) in 20–40 keV was obtained as 2.4 arcmin, which is slightly worse than 1.9 arcmin measured at 4.51 keV. The difference is due to the energy dependency of the amplitude of scattering tails, which is higher in shorter wavelength(e.g., Tsusaka *et al* 1995). The core broadening inside of 1.5 arcmin diameter is almost identical for hard and soft X-rays, implying that the spatial resolution of the demonstrational model is as good as *ASTRO-E* XRT, which is expected to be about 0.5 arcmin. The detailed description about the experiment is also seen in Yamashita *et al.* (1998b).

3. INFOCμS : BALLOON-BORNE HARD X-RAY TELESCOPE MISSION

3.1. Mission concept

International Focusing Optics Collaboration for μCrab Sensitivity (InFOCμS) is a balloon-borne hard X-ray telescope observation project. The project is initiated by NASA Goddard Space Flight Center. The hard X-ray optics consists of supermirror-coated thin foil conical mirror telescope and CdZnTe pixel imaging detector. Two types of mirror

	Telescope	
	Low Energy Mirror	High Energy Mirror
Energy bandwidth	20-40 keV	65-80 keV
Number of units	1	3
Diameter/Focal length	40 cm/8.0 m	30 cm/8.0 m
Effective area (one telescope)	100 cm^2	50 cm^2
Field of view	10 arcmin	2-3 arcmin
Half power diameter	1.5-2 arcmin	1.5-2 arcmin
Mirror surface	multi block supermirror	TBD
	Focal Plane Instrument	
Detector	CdZnTe pixel detector	
Position resolution	380 μm (pixel pitch)	
Efficiency	100% @20-40 keV, $\geq$95% @65-80 keV	

Table 1. Design parameters of InFOCμS mission. Parameters for High Energy Mirror are tentative.

systems are planned; the Low Energy Mirror for 20–40 keV observation and the High Energy Mirror for 60–80 keV band.

Table 1 shows design parameters of main payload instruments of the mission. The telescope optics is basically the similar systems as *ASTRO-E* XRT but with longer focal length. Their mirror shells are the epoxy-replicated conical foil mirrors. The reflecting surfaces are equipped with multilayers with graded periodic length to achieve hard X-ray sensitivity. The development of multilayers is a joint study by Nagoya University and NASA/GSFC. The first flight is scheduled in the summer of 2000.

3.2. Telescope design and fabrication

One set of the Low Energy Mirror and the focal plane CdZnTe imager is planned to fly in the first flight. The diameter of the telescope is 40 cm and the focal length is 8 m, thus angles of incidence (θ) are from 0.11 to 0.36 deg for 256 nested mirror shells.

The reflectors are currently being fabricated at both of Nagoya University and NASA/GSFC. The reflectors are fabricated in two ways; supermirror deposition onto pre-replicated platinum mirrors by Nagoya team and direct replication of supermirrors deposited onto mandrel by GSFC team. The direct replication of supermirrors is newly developed and well established technique (e.g., Ogasaka *et al.* 1998, Furuzawa *et al.*, 1998, also Owens *et al.* in this proceedings). This part of the paper is mainly dedicated to report and discuss the current status at Nagoya. The status of GSFC production is described by Owens *et al.* in this proccedings.

The supermirrors were designed so that every single reflector covers entire energy region of 20 to 40 keV. As described in section 2.1, designing is based on the multi-block method. Except for very outer ones, most of the reflectors have relatively thick (2.0 to 4.0 nm) platinum layer on top of a supermirror, which we call "top coating", in order to enhance reflectivity towards low energy end. This is effective because, with such small angles of incidence for these reflectors, total external reflection by single layer of platinum is still usable up to about 30 keV. Figure 3 shows an example of supermirror thus designed. This design consists of six blocks of 41 layer pairs in total, with 4.0 nm-thick platinum top coating. Layer thickness (d) varies from 3.6 to 6.6 nm. The design shown in this figure covers energy region well below and above the region of interest (20-40 keV). For off-axis X-rays, angles of incidence shift off the nominal, which is equivalent to the change of energy under the Bragg condition of multilayers. Therefore, to cover wide range of incidence angles, energy response (or angular response) of supermirror needs to be wider than nominal.

To accommodate with 256 different incidence angles, 13 different sets of supermirror designs are prepared. The layer thickness is from 3.0 to 9.0 nm. About 20 foils fall into one group, all of which are coated with supermirrors of identical design. Range of incidence angles in one group is less than 10 %. Design parameters of all 13 groups are shown in figure 4, in terms of effective areas of each group. Overlaid is the sum of them, that is, the total effective area as a telescope. There are slight differences of energy range covered by each group, but the region of 20 to 40 keV is securely covered by all groups.

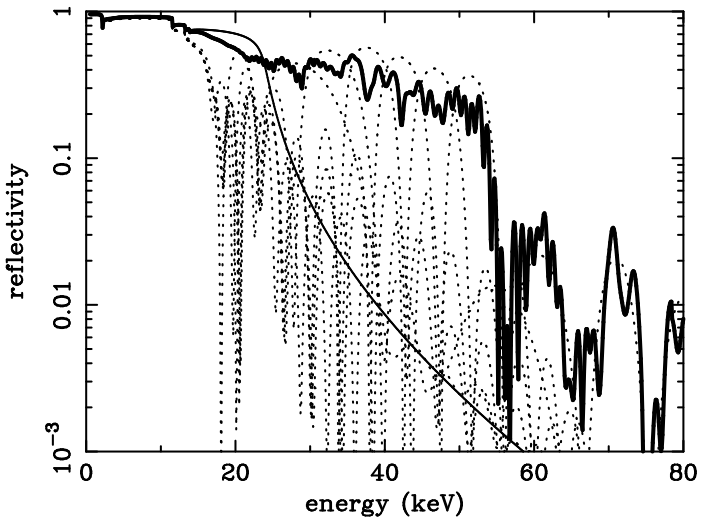

Figure 3. Example of InFOCμS supermirror model reflectivity (thick solid line). Six blocks (dot lines) are stacked as well as 4.0 nm of platinum top coating (solid line), to cover 20 to 40 keV region. At the incidence angle of 0.201° for this case, single layer of platinum still has enough reflectivity up to about 25 keV. Total number of layer pairs is 41, and layer thickness (d) is from 3.6 to 6.6 nm.

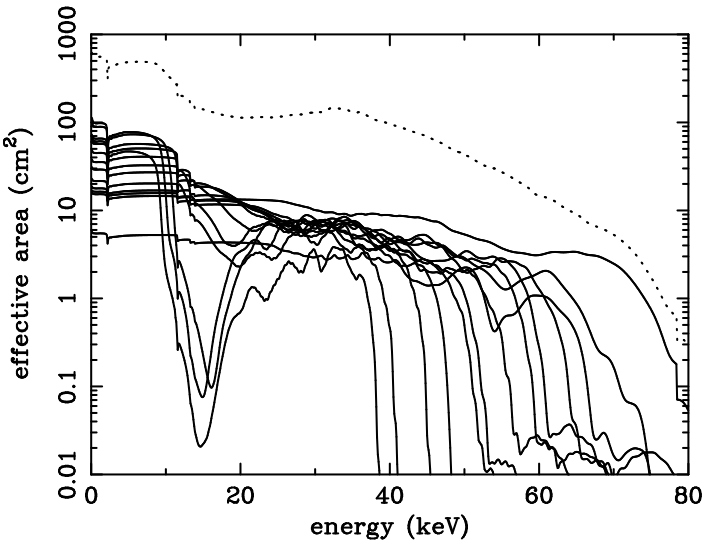

Figure 4. Effective areas of each foil groups (solid lines) and of telescope (dashed line). Among 13 groups, inner 10 groups have platinum top coating and their effective areas have smooth continuation to lower energy. 3 groups (lines with dip at 15 keV) are of outermost ones, where total external reflection by platinum single layer is no longer effective since incidence angles are large.

3.3. X-ray characterization of reflectors

3.3.1. X-ray reflectivity

The X-ray characteristics of fabricated foils were measured with pencil X-ray beam. Figure 5 is an example of a reflectivity of supermirror fabricated on platinum replica foil mirror, measured with 8.0 keV monochromatic X-rays. The overlaid model calculation assumes interfacial roughness of 0.35 nm. This value is comparable to that of the substrate platinum surface, indicating that our supermirror deposition is successful.

Fabricated foil mirrors must be evaluated at X-ray energies where they will be actually used. For this purpose, we carried out a series of hard X-ray measurements at high brilliance synchrotron facility, SPring-8 in Japan (figure 7). This experiment is a joint program of Nagoya University and Himeji Institute of Technology. The schematics of the experiment setup (BL24XU Hatch C) is shown in figure 8. Figure 6 shows angular reflectivity of the same supermirror shown in the figure 5, measured at 32 keV. This sample shows a flat-top reflectivity of about 30 % from 0.25 to 0.35 degrees. Overlaid model calculation assumes interfacial roughness of around 0.30 nm, which is quite satisfactory.

3.3.2. Scattering tails

Another key feature of X-ray reflectors coated with supermirror is their unique distribution of scattered X-rays. Because of their periodic structures along depth direction, non-specular scattered X-rays have higher power than those from reflectors with single layer. The principle of such scattering tail due to "correlated roughness" is similar to that of multilayer-enhanced reflection gratings. In the case of multilayer gratings, enhancement of non-specular reflection is observed where both of Bragg condition of multilayer and diffraction condition of grating is satisfied.

The left panel of figure 9 shows measured profiles of scattered X-rays of a multilayer. When measured at the incidence angle which satisfies Bragg condition, scattered power distributes in very similar way to single layer mirror. However, when the incidence angle is slightly off from the Bragg peak, an enhancement is observed in the region of scattered tails. The location of such non-specular enhancement is where general form of Bragg condition is satisfied. With perfect boundary of a multilayer, such non-specular component is wiped out due to interference along the direction parallel to the surface. In practice, interfaces, as well as surfaces, have various frequency components of roughness. Then, selected frequency "correlated" to the periodic structure along depth direction interferes with scattered X-rays.

These enhancements may produce significant non-specular power, thus considerable amount of stray lights could be produced. The qualitative evaluation is currently under study, but as seen from the right panel of figure 9, the amplitude of such enhancement is relatively small comparing to on-Bragg, specular power. This is because that even though the amplitude of such enhancement may be comparable to that of specular peak, the total scattered power is very small since incidence angle is off-Bragg. Roughly speaking, amplitude of such enhancements are reduced by the ratio of off-Bragg to on-Bragg reflectivity. Therefore, there may not be so much chance for these enhancements to distort focused image significantly.

Figure 10 presents the same measurement as data (c) in figure 9 but of supermirror deposited on platinum replica mirror. The enhancement from 0.3 to 0.8 deg originated from second order Bragg peaks has little impact on imaging capabilities, from the reason described above. However, due to the nature of a supermirror, enhancement produced by first order Bragg peaks clusters around specular peak. This may cause non-negligible distortion of focused image. Our current estimate indicates that they still have very small contribution to stray lights, but further study is important and necessary.

The analysis of these non-specular structures is important not only to understand the focusing characteristics of hard X-ray telescope, but also to evaluate conditions of layer boundaries, that is, interfacial roughness and inter-diffusion. This is because reduction of reflectivity is a function of both conditions, while non-specular enhancement depends mostly on interfacial roughness. We are currently working on this issue (Ichimaru *et al.* 2000, in preparation), and the result will be reported in the near future.

3.4. Sensitivity

Figure 11 shows model effective area of InFOCμS telescope. The periodic lengths of supermirrors are from 3.0 to 9.0 nm while interfacial roughness we have been observing so far is from 0.35 to 0.40 nm. Therefore, reflectivity

of a supermirror is very sensitive to their interfacial roughness. At the interfacial roughness of 0.40 nm , expected effective area in 20 to 40 keV region is about 100 cm^2 or slightly less.

Figure 12 presents the expected detection limit of InFOCμS telescope for faint sources, in comparison to the past experiments. For entire energy region of InFOCμS Low Energy Mirror, sensitivity is background limited. In 20–40 keV region, the sensitivity is improved by about one order of magnitude comparing to past experiments. Assuming power law spectrum with energy index of -0.7, the detection limit of InFOCμS telescope is comparable, when scaled by source spectrum, to several times 10^{-13} erg s^{-1} cm^{-2} in 2–10 keV.

Figure 13 shows a simulated spectrum of InFOCμS observation of 3C273, a quasar at $z = 0.16$, with 20 ksec exposure. It depends on the zenith angle of pointing direction, but in general, X-rays below 20 keV is severely absorbed.

4. FUTURE PLANS

The future InFOCμS flights are planned to carry High Energy Mirrors which focus hard X-rays above 60 keV. The design of supermirrors for such high energy use may not be simple nor straightforward. To obtain high aperture efficiency as Low Energy Mirror, telescope diameter and focal length, or their ratio, are better to be unchanged. Then, extremely small periodic length is required while our current technology is not enough to achieve it. One idea is to utilize higher order Bragg peaks, as discussed by Yamashita *et al.* (1999).

Japanese future X-ray astronomy mission *ASTRO-G* (name is not official approved yet) is now under conceptual study. For X-ray telescopes, wide-band sensitivity from 0.5 to 100 keV is requested. The main scientific objective of the mission is to investigate the mechanisms of acceleration in the Universe. The thin-foil supermirror-enhanced X-ray telescope described in this paper is quite suitable for the mission, although some technological innovation is required. For example, current imaging capability is somewhat insufficient for multi-purpose observatory in the future. Also, supermirrors having sensitivity beyond 40 keV is still under study. Throughout InFOCμS program, we hope to achieve technological breakthrough for the future.

ACKNOWLEDGMENTS

This work has been supported in part by a Grant-in-Aid for Scientific Research on Specially Promoted Research, contract No. 07102007, from the Ministry of Education, Science, Sports and Culture, Japan. YO acknowledges the support from the Research Fellowships of the Japan Society for the Promotion of Science.

REFERENCES

1. Cappi, M. *et al.*, 1998, *Publ. Astron. Soc. Japan*, **50**, 213.
2. Furuzawa, A. *et al.*, 1998, *Proc. SPIE*, **3444**, 576.
3. Ichimaru, S. *et al.* 2000, *in preparation.*
4. Ogasaka, Y. *et al.*, 1997, *Bulletin of the American Astronomical Society*, **29**, 1305.
5. Owens, S. *et al.*, 2000, *this proceedings.*
6. Serlemitsos, P. J. *et al.*, 1995, *Publ. Astron. Soc. Japan*, **47**, 105.
7. Tawara, Y. *et al.*, 1997, *Proc. SPIE*, **3113**, 285.
8. Tsusaka, Y. *et al.*, 1995, *Appl. Opt.*, **34**, 4848.
9. Yamashita, K. *et al.*, 1998a, *J. Synchrotron Rad.*, **5**, 711.
10. Yamashita, K. *et al.*, 1998b, *Appl. Opt.*, **37**, 8067.
11. Yamashita, K. *et al.*, 1999, *Proc. SPIE*, **3766**, 327.

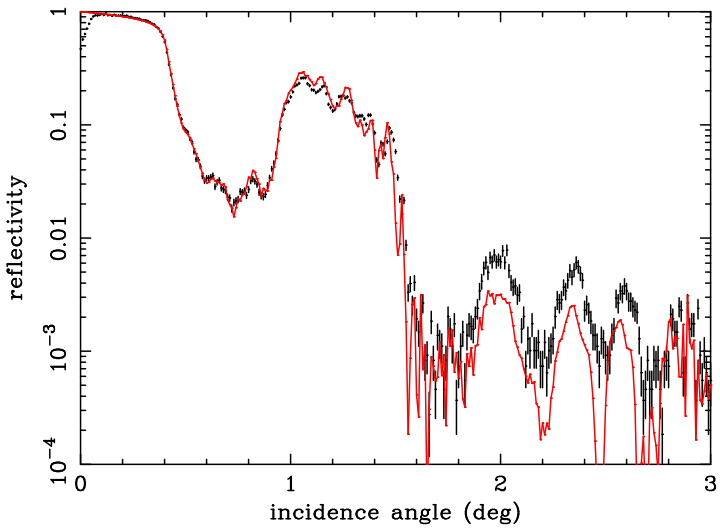

Figure 5. Reflectivity of a supermirror deposited on platinum replica foil mirror, measured at 8.0 keV (dot with error bars). Overlaid model (solid line) assumes interfacial roughness of 0.35 nm, showing excellent fit to the data for total reflection region and first order Bragg peak complex. The structure of the supermirror is; (d(nm), N) = (4.7, 1)(4.6, 1)(4.5, 1)(4.47, 1)(4.43, 1)(3.85, 8)(3.5, 12)(3.2, 18)(3.1, 25). Γ is fixed to 0.43.

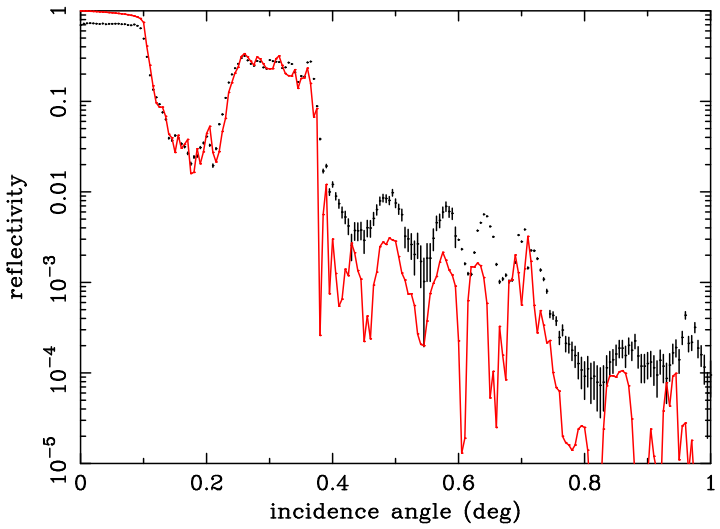

Figure 6. Reflectivity of the same sample as in figure 5 measured at 32.0 keV (dot with error bars). Overlaid model (solid line) assumes interfacial roughness of 0.30 nm.

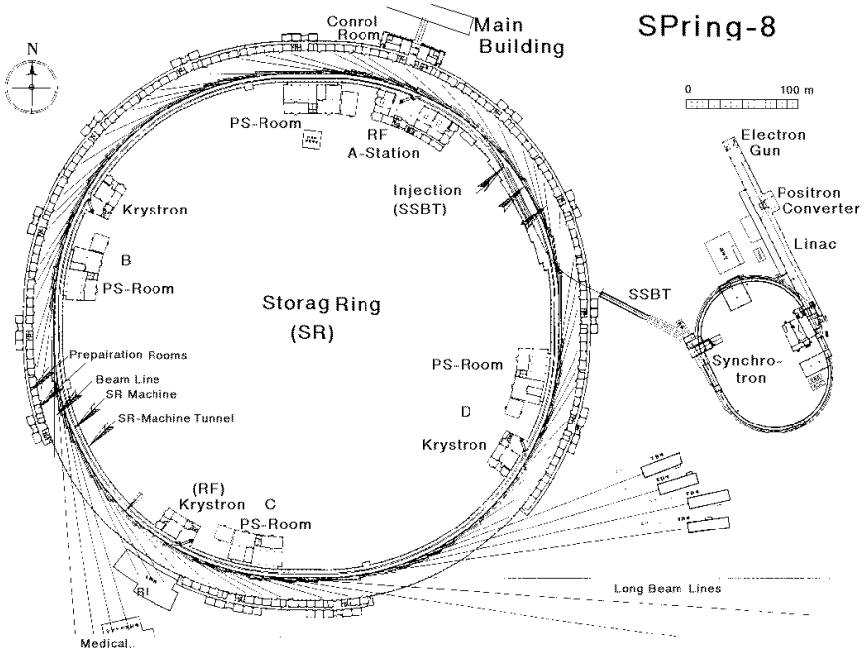

Figure 7. The overview of SPring-8 Storage Ring (SR) and accelerators. Diameter of the ring is about 450m. The gap energy and the maximum current are 8 GeV and 100 mA, respectively.

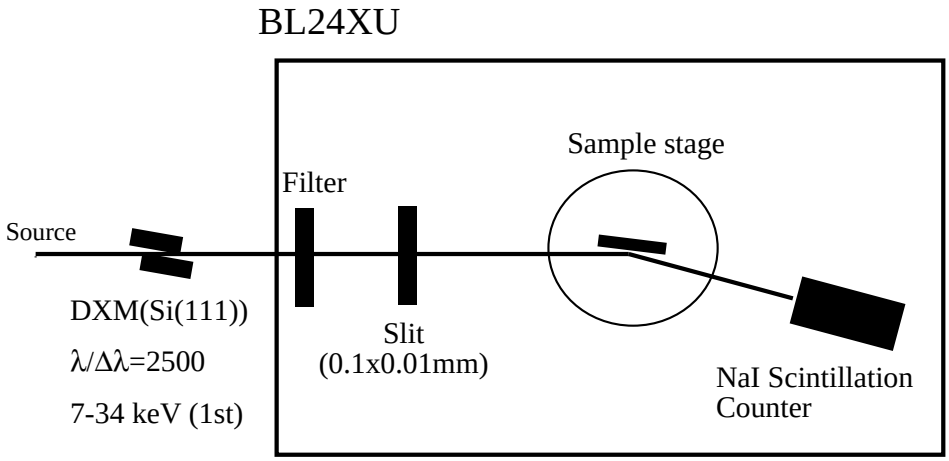

Figure 8. Schematics of the experimental setup at SPring-8 BL24XU (Hyogo Beam Line) Hatch C. The monochromatic X-rays are introduced to the Hatch (solid box), and then filtered to reduce beam flux so that samples are not damaged. X-rays are collimated by 0.1 (vertical) $\times$ 0.01 (horizontal) mm^2 slit. The flux of incident beam is 10^5 to 10^6 counts s^{-1} depending on the choice of X-ray energy.

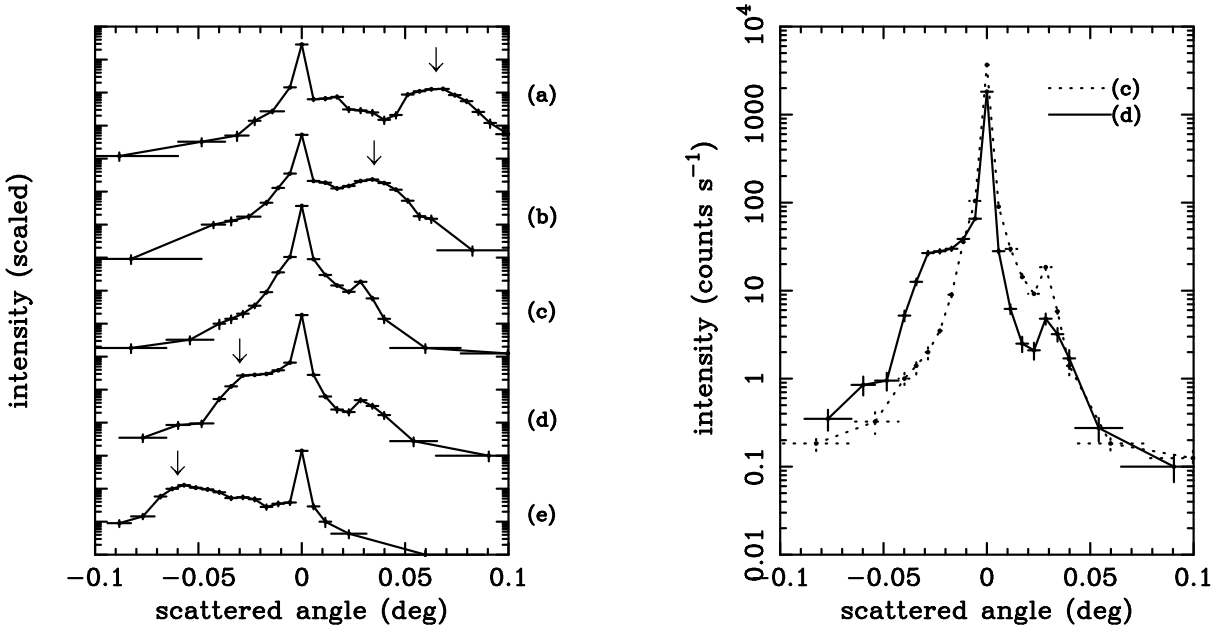

Figure 9. Measurement of scattered tails of a multilayer ($d = 3.76$nm, $N = 20$, $\Gamma = 0.43$) at different incidence angles (θ_{in}) near first order Bragg peak. Data was obtained at SPring-8 using monochromatic 32 keV X-rays. $\theta_{in} = 0.317°$ for first order Bragg peak. Left panel: scattered profiles for $\delta\theta_{in}$(angle from Bragg peak) $= -0.032°$(a), $-0.017°$(b), $0.0°$(c), $+0.018°$(d), $and + 0.028°$(e). The arrows indicate the enhancement due to the correlated roughness as described in the text. Right panel: Comparison of the amplitude of scattered structures for on- and off-Bragg profiles. The legends indicate the same θ_{in} as the left panel.

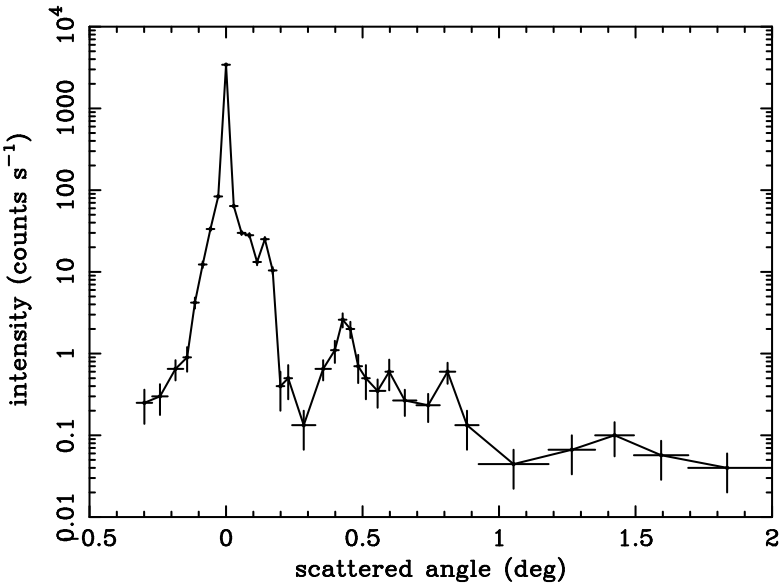

Figure 10. The scattered profile of the supermirror as described in figure 6. The enhancement accompanied by sharp specular peak is a result of lateral roughness structure correlated to layer structure. The Bragg condition satisfied at this region of scattered angle corresponds to that of first order Bragg peak complex as seen in the right panel of figure 6. The enhancement seen in 0.3–0.9° corresponds to second order Bragg peaks.

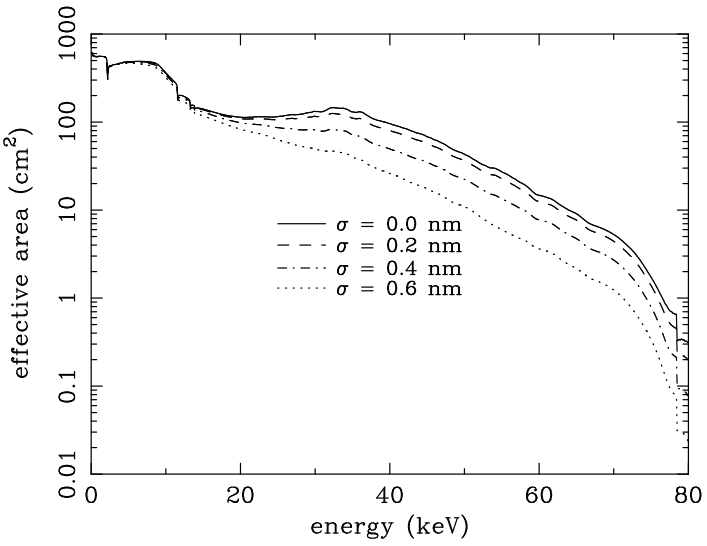

Figure 11. Effective area of InFOCμS telescope for various interfacial roughness (σ) of supermirrors.

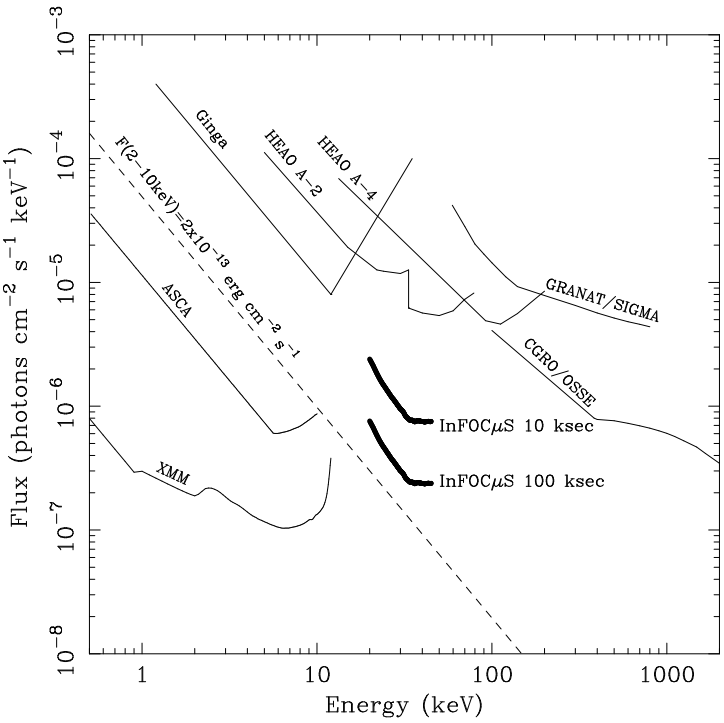

Figure 12. Detection limit of InFOCμS 2000 Summer flight for 10 and 100 ksec exposure, with comparison to the past experiments. All the past experiments above 10 keV are non-imaging detectors. A sharp upturn of InFOCμS detection limit towards low energy end is partially due to atmospheric absorption at the balloon altitude of 40 km.

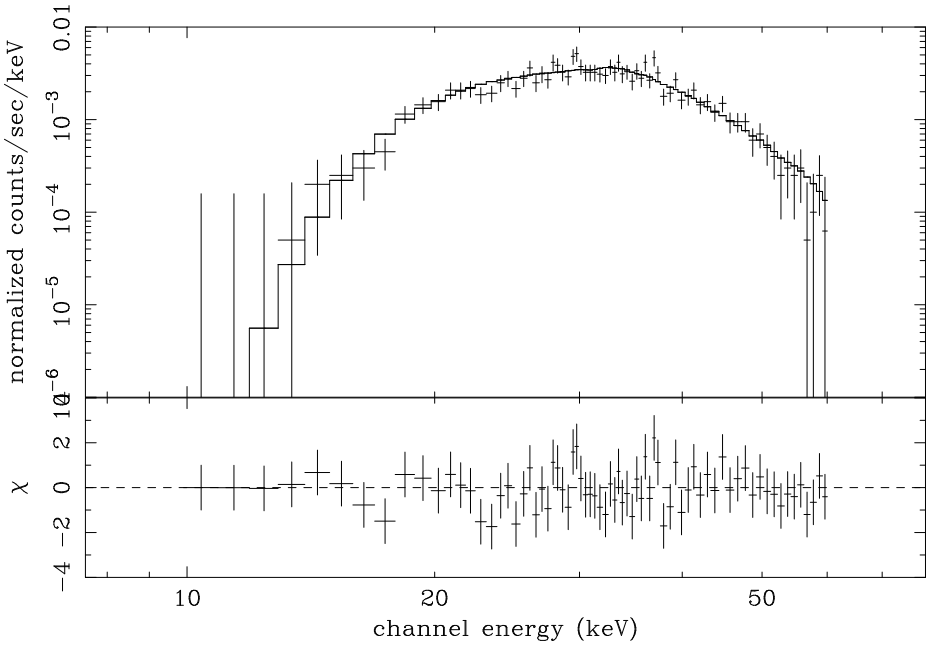

Figure 13. Simulated spectrum of 3C273 for 20 ksec observation. The parameters for source spectrum were adopted from Cappi *et al.*, 1998.